Ab Initio Calculations of ^{17}O NMR-Chemical Shifts for Water. The Limits of PCM Theory and the Role of Hydrogen-Bond Geometry and Cooperativity

Roger A. Klein*

Institute for Physiological Chemistry, University of Bonn, Nussallee 11, D-53115 Bonn, Federal Republic of Germany

Benedetta Mennucci† and Jacopo Tomasi‡

Department of Chemistry and Industrial Chemistry, University of Pisa, Via de Risorgimento 35, I-56126 Pisa, Italy

Received: March 22, 2004; In Final Form: May 3, 2004

We demonstrate here that it is possible to calculate with reasonable accuracy the ^{17}O-chemical shift for the gas-to-liquid phase change for water using density functional theory (DFT) and water clusters in which both cluster size and cooperative hydrogen bonding are taken into account. Cooperative hydrogen bonding in a highly structured, tetrahedrally symmetric environment results in ^{17}O-chemical shifts sufficient to mimic the change from monomeric water in the gas phase to that in high-pressure ice. We also show that polarizable continuum models (PCM) using a self-consistent reaction field (SCRF) fail to predict adequately ^{17}O-chemical shifts for water in the condensed liquid or solid phase, discussing this problem in terms of any solute−solvent system in which there is cooperative charge transfer. This is believed to be the first report analyzing the ^{17}O-chemical shielding tensor behavior in water clusters explicitly as evidenced by electron density topology of the hydrogen bonds, NBO antibonding orbital occupancies, electric field gradients, and full electrostatic multipole analysis for the oxygen and hydrogen atoms, thus providing an insight into the failure of the polarizable continuum model to describe liquid water accurately.

Introduction

The accurate determination of the ^{17}O-chemical shielding tensor for water molecules in the liquid state by ab initio computational methods places severe demands on both the electron correlation procedure used and the model of how individual H_2O molecules interact with one another.

The change in state for water from the gas phase to the liquid phase is associated with a step change in ^{17}O NMR-chemical shift of +36.1 ppm; the chemical shift temperature sensitivity between 100 and 0 °C is approximately linear with a temperature coefficient of -0.0435 ± 0.0007 ppm/°C, giving another +4.35 ppm (own unpublished results); and finally the transition from liquid to ice gives rise to a further +8 ppm[1] (and references quoted therein). Any method of calculation and the water model used must be able to take account not only of the difference in chemical shift between the gas and liquid phase but must also be able to predict the order of magnitude of the temperature sensitivity. Increasing chemical shift, that is, the reduction in the isotropic chemical shielding tensor, with an increasingly ordered or structured state on passing from vapor to liquid and thence to ice, is related to the average degree of hydrogen bonding for the water molecules, averaged over time and space, up to the maximum possible of two donor and two acceptor ligand valencies per water being satisfied.[2] The marked directionality of hydrogen bonding for water is determined by the approximately tetrahedrally symmetric arrangement of the two O−H covalent bonds and the two lone-pair electrons.

Several theoretical approaches have been proposed for treating nuclear magnetic shielding in solution.[3] These approaches can be classified broadly into two types: continuum models[4] and molecular dynamics simulations using either classical or ab initio formulations.[5]

The continuum model approach has been used to evaluate various molecular properties in solution[6] and has given reasonable agreement with experimental data. A more demanding situation is the calculation of the nuclear magnetic shielding: this is a microscopic property that is highly sensitive not only to the structure of the molecule in question but also to intermolecular interactions such as hydrogen bonding. The description provided by the continuum solvent model may miss parts of the microscopic processes occurring in solution[7] and thus only accounts partially for the solvent-effect on nuclear shielding, or may even lead to the wrong conclusions.[8]

The approach based on molecular simulation seems to be promising as a means of studying NMR chemical shifts in solution, because it can take molecular details of the solvent into account by sampling the conformational equilibrium. In a recent study, NMR chemical shifts have been obtained by carrying out ab initio calculations for a few molecular clusters selected from the configurational space sampled by the molecular simulation.[9] The approach is attractive because the intermolecular interactions can be treated quantum mechanically. More recently, this kind of approach has been refined further by adding a continuum solvent to the solute−solvent clusters so as to account also for long-range effects.[8,10]

The same solvation methods have also been applied to the complex case of oxygen nuclear shielding of water in water. In

* Corresponding author. E-mail: klein@institut.physiochem.uni-bonn.de.
† E-mail: bene@dcci.unipi.it.
‡ E-mail: tomasi@dcci.unipi.it.

10.1021/jp0487408 CCC: $27.50
Published on Web 06/16/2004

particular, estimating the gas−liquid-phase shift for the ^{17}O nucleus in water using continuum methods has not been particularly successful as the calculated shifts are in the wrong direction for oxygen, although they are reasonable for hydrogen.[11] As pointed out recently by Cramer,[12] a specific problem of all current continuum models, and one that is related to the problem of charge penetration into the solvent, is that there is at present no mechanism available capable of taking into account charge transfer between the solute and solvent molecules. This problem is likely to be particularly acute when one considers a water molecule embedded in solvent water as part of a highly cooperative water cluster in which each water molecule can act simultaneously as both a hydrogen-bond donor and acceptor.

Molecular dynamics methods have been more successful. There have been many attempts to calculate the change in the chemical shielding tensor for ^{17}O and for ^{1}H on passing from the gas phase to the liquid phase, or even solid-phase ice. Perhaps the most successful study to date is that of Pfrommer et al.,[13] in which Car-Parrinello molecular dynamics (CPMD)[14] were used to model the behavior of bulk water.

We have approached this problem from a different, more reductionist viewpoint, choosing to model long-range order in liquid water and ice explicitly by investigating a range of defined water clusters or super-molecules of differing size ($n = 1-23$) with known geometry and hydrogen-bond cooperativity, defined as the interaction between water molecules acting as both hydrogen-bond donors and acceptors in an alternating fashion. The flickering cluster model for liquid water is well-established based on both theoretical and experimental studies as an explanation for the physical properties and long-range structure of water.[15] Neutron diffraction data show that water at room temperature has a radial distribution function indicating some degree of structuring out to the third or fourth hydration layer.[16] Moreover, high-pressure ice or water cages in gas clathrates show an even greater degree of long-range structuring,[17] based mainly on pentagonal rings rather than hexagonal rings as is considered to be the case for liquid water.

We show in this paper that not only is cluster size important but also the average occupancy of the four possible hydrogen-bond ligand "valencies" is critical in one's ability to predict accurately the gas-to-liquid ^{17}O-chemical shift using computational methods.

Methods

All optimizations and subsequent calculations were carried out originally using Gaussian 98 (revision A.11 25-Sep-2001)[18] at the MP1PW91/6-311+G(2d,p) level of theory and were repeated with Gaussian G03 (revision B.05 3-Mar-2003)[19] for the natural chemical shielding analysis (NCSA)[20] and the IEFPCM calculations. Chemical shift values obtained with G98 and G03 agreed within ±0.1 ppm (see below). Use of the hybrid density functional MPW1PW91 in conjunction with the 6-311+G-(2d,p) basis set has been shown previously to give reliable NMR and geometrical results for moderate-sized hydrogen-bonded systems at realistic computational cost,[21−23] the diffuse and polarization functions being essential. Wave function files were generated in Cartesian coordinates (6D 10F) and then analyzed further for electron density topology using AIM2000[24] and Morphy98[25] software. Natural bonding orbital (NBO) analysis was carried out on the file generated from the Gaussian option pop=NBOread, using version 5 of the Wisconsin NBO program.[20] NMR chemical shielding tensors were calculated by the method of gauge-including atomic orbitals (GIAO), based on the original methods of Ditchfield and Hameka,[26] as implemented for density functional theory (DFT) in the Gaussian software; chemical shielding anisotropy and asymmetry parameters were calculated from the individual eigenvalues.

Differences in Behavior between the Hybrid DFT Functionals MPW1PW91(g98) and MPW1PW91(g03). The hybrid DFT functional MPW1PW91, and others related to Perdew and Wang's PW91, has been modified in G03 as compared to G98 in its treatment of the local scaling factor. MPW1PW91(g98) is still available within G03 as OMPW1PW91 (Gaussian, Inc. Release Notes for G03 Revision B.05 3-Mar-2003).

We have compared the behavior of MPW1PW91(g98) and MPW1PW91(g03) for an extensive series of water clusters, including tetrahedrally coordinated water. G03 gives ^{17}O NMR-chemical shielding tensors that are, on average, +0.070 ppm (±0.071) high as compared to G98. This difference is not significant and falls within the typical spread seen for apparently magnetically equivalent nuclei in clusters of approximately ±0.3 ppm. ^{1}H-chemical shielding tensors for hydrogen-bonded hydrogens differ by +0.012 ppm (±0.012) and for non-hydrogen-bonded hydrogens by +0.006 ppm (±0.003), an order of magnitude lower than for ^{17}O, differences that are again insignificant as compared to a "realistic" error of ±0.1 ppm. The differences in hydrogen-bond geometry are also insignificant; MPW1PW91(g03) yields O···H donor−acceptor distances that are, on average, +0.00065 Å (±0.00081) longer than those for MPW1PW91(g98).

The calculated energies of the final structures, but not the final geometries or the chemical shifts which are both virtually identical, are, however, significantly different. MPW1PW91-(g03) gives energies that are consistently more negative, that is, apparently more stable but caused basically by an algorithm artifact, by -0.284 ± 0.029 kcal/mol/H_2O molecule in our complete series of clusters. It must be stressed that the G98 and G03 structures are identical geometrically within calculation error. Thus, MPW1PW91(g03) and MPW1PW91(g98) energies should not be compared directly, as this will give physically meaningless differences.

Water Clusters. The following structures were investigated: (i) the water monomer; (ii) the water dimer; (iii) the trimers consisting of a central water molecule hydrogen bonded as either a double acceptor (3(2A)) or a double donor (3(2D)) to two other isolated water molecules, or in the form of a cooperative ring (3R); (iv) tetramers consisting of a ring (4R), a bicyclic cage (4B), or a cyclic trimer with an additional water molecule hydrogen bonded as either a donor (4D) or an acceptor (4A); (v) pentamers in the form of a symmetrical pentagonal ring (5R), an open or "naked" tetrahedron with a tetrahedrally symmetric (5T), central coordinated water molecule, or as two fused cyclic trimers (5Tw); (vi) a hexagonal ring; (vii) a symmetrical cubic octamer; (ix) a decamer consisting of three interlocking pentagonal rings; (x) an undecamer consisting of three pentagonal rings fused along one edge; (xi) a tridecamer made up of six cyclic trimers and containing five four-coordinated oxygen atoms; (xii) a heptadecamer consisting of six interlocking pentagonal rings with five equivalent sp^3-coordinated oxygen atoms; (xiii) an eicosamer cage made up of 12 pentagonal pentamer rings equivalent to the 5^{12} sI methane-clathrate water cage,[27] and a tetracosamer $5^{12}6^2$ cage − details for the clathrates will be reported in detail in a subsequent publication (Klein and Zottola, to be published); (xiv) a symmetrical tricosamer consisting of nine interlocking pentagonal rings with eight equivalent sp^3-coordinated oxygen atoms; (xv) a series of two equally sized rings fused at a central water molecule (ring size, $n = 3-6$; giving a $[2n - 1]$-mer).

SCHEME 1: Structures of the Most Important Water Clusters Studied[a]

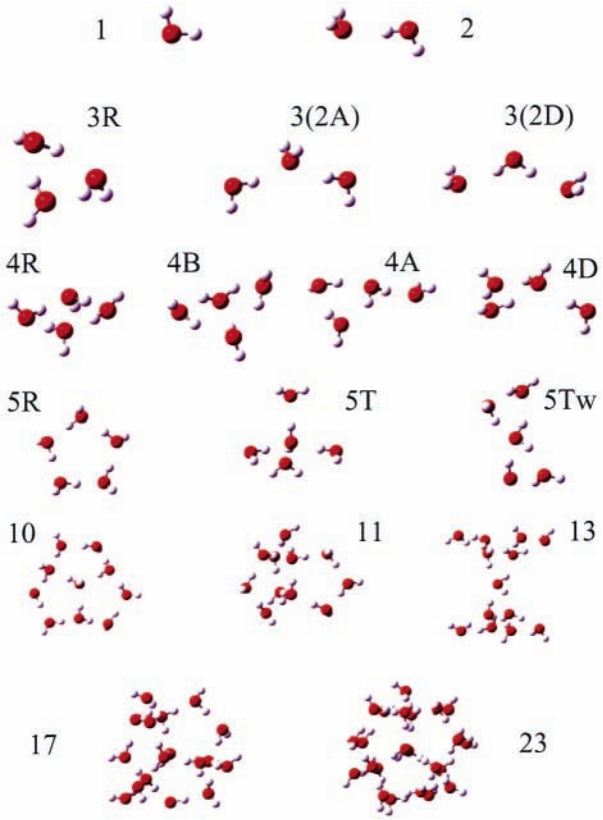

[a] The following are shown: the water monomer (1); the dimer (2); the ring trimer (3R); the trimer with the central water molecule acting as a bi-acceptor (3(2A)) or bi-donor (3(2D)); the ring tetramer as a symmetrical, planar ring (4R) and as a folded ring (4B); the tetramer consisting of a ring trimer with an external acceptor (4A) or donor (4D) water molecule; the ring pentamer (5R); the pentamer with a central tetrahedrally four-coordinated water (5T); the twisted pentamer consisting of two fused ring trimers (5Tw); the decamer consisting of three edge-fused pentagonal rings in the form of a "cap" (10); the undecamer made up of three pentagonal rings fused along one common edge (11); the tridecamer consisting of six ring trimers fused at four-coordinated waters (13); the heptadecamer (17) and tricosamer (23) consisting of six and nine edge-fused pentagonal rings, respectively.

The structures are shown as molecular models in Schemes 1 (for systems i−v, x−xii, and xiv), 2 (for system xv), and 3 (for system xiii); the Arabic numeral in each case refers to the number of water molecules in the cluster, qualified by a letter if there is more than one isomeric structure shown.

We chose to investigate large clusters made up of interlocking pentagons, rather than hexagons, for the following reasons. First, the ^{17}O-chemical shift change in open-ring systems with each water molecule acting as a single hydrogen-bond donor and single hydrogen-bond acceptor has virtually reached a plateau by $n = 5$. Second, interlocking quasi-planar pentagons give almost pure sp^3 tetrahedral symmetry ($\theta_{sp3} = 109.47°$ as compared to $\theta = 108°$ for a pentagon) for water molecules with all four hydrogen-bond "valencies" satisfied (two donor and two acceptor, i.e., 2D/2A). Third, pentagons are more computationally efficient for large clusters, minimizing the ratio of the number of water molecules to the number of tetrahedrally, cooperatively coordinated oxygen atoms and hence the number of basis functions needed with the associated scaling problem; for example, the 11'mer with two tetrahedrally coordinated, central oxygen atoms would require 14 water monomers if made up of hexagons, the 17'mer with five, $n = 23$, and the 23'mer

SCHEME 2: Clusters Containing Two Equal-Sized Ring Systems Fused at a Single, Tetrahedrally Coordinated Water Molecule, Showing the Pentamer, Heptamer, Nonamer, and Undecamer with, Respectively, Ring Sizes of 3, 4, 5, and 6

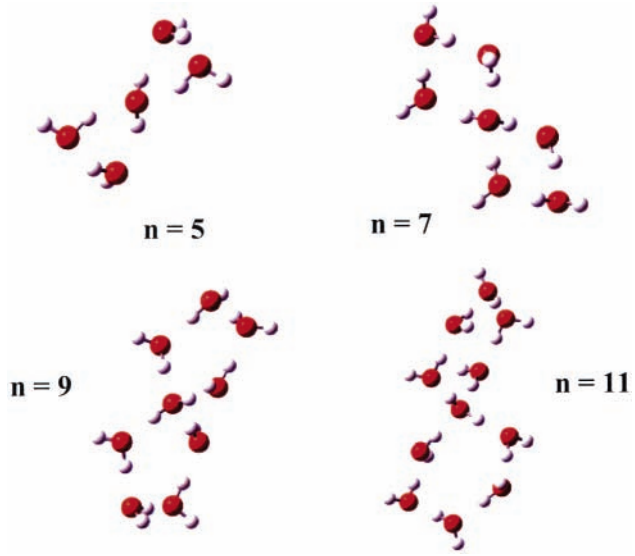

with eight, $n = 32$, respectively. Fourth, the radial distribution function for oxygen in $(\text{pentamer})_n$ clusters is very similar to that for hexagonal phase ice[16] as far as the second coordination shell is concerned, $1.60d$ and $1.63d$, respectively, where d is the nearest, first shell O−O spacing and mimics accurately that for methane-clathrates,[17] in which we are also interested (Klein and Zottola, unpublished work).

Results

NMR Chemical Shift. We have calculated the chemical shielding tensors for ^{1}H and ^{17}O for water in a series of $(H_2O)_n$ clusters from $n = 2$ to $n = 23$, at the MPW1PW91/6-311+G-(2d,p) level of theory. The value of the ^{17}O-shielding tensor we obtained for the water monomer in the gas phase of 327.3 ppm is in excellent agreement with the asymptotic value at the CCSD(T)/cc-pVXZ level, without rovibrational corrections, of 327.7 ± 0.3 ppm reported by Vaara, Lounila, Ruud, and Helgaker.[28] These authors propose an absolute value of 324.0 ± 1.5 ppm corrected for rovibrational effects at 300 K, based on earlier work referenced to carbon monoxide and referred to in their paper. Our MPW1PW91/6-311+G(2d,p) value of 31.71 ppm for the water proton is, however, somewhat higher than their CCSD(T)/cc-pV6Z value of 30.47 ppm.

Figure 1 shows the ^{17}O-chemical shielding for the range of water clusters investigated plotted against a "coordination index". The coordination index is defined by a cardinal number to the left of the decimal point representing the number of hydrogen bonds in which the water molecule is involved, that is, the sum of the donor $H_D\cdots O$ and acceptor $O_A\cdots H$ interactions, and a number to the right of the decimal point indicating cooperativity. For example, a coordination number of 3.2 would indicate that three of the four possible valencies were filled − no distinction is made between 2A/1D or 1A/2D although there are small, systematic differences observed − with the number after the decimal point indicating the degree of cooperativity; that is, 0 = an open-chain system with no donor−acceptor cooperativity, 2 = cooperativity but within a strained three-ring system, and 4 = cooperativity within an unstrained ring system ($n \geq 4$). It must be stressed that the use of this

SCHEME 3: The Clathrate-like eicosamer (5^{12}) and Tetracosamer ($5^{12}6^2$) Clusters Consisting of Edge-Fused Pentagonal Rings with All of the Water Molecules Three-Coordinated, That Is, Either Acting as Two Hydrogen-Bond Donors and One Acceptor, or One Donor and Two Acceptors, Projected along Their Axis of Symmetry

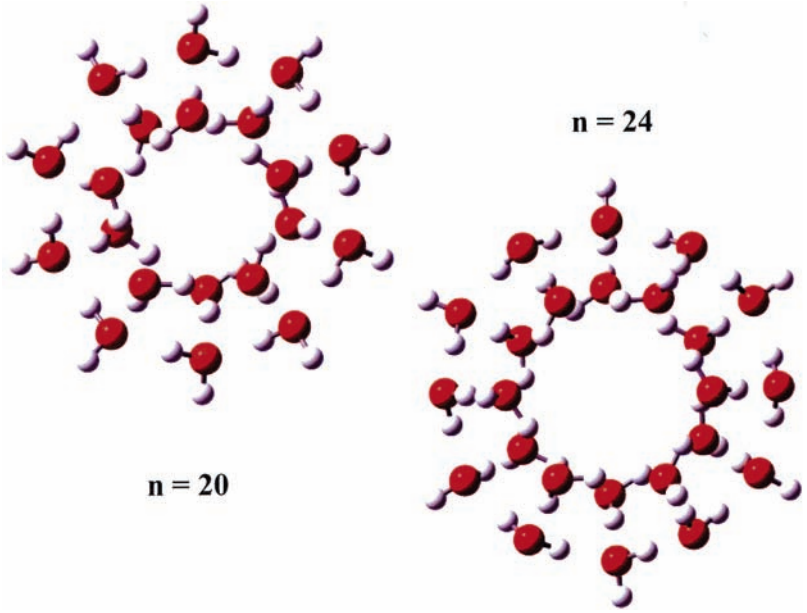

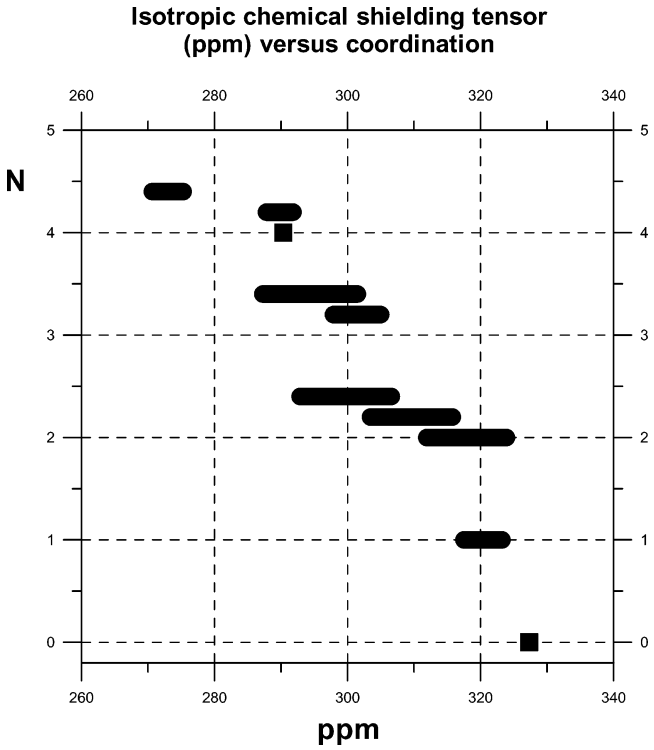

Figure 1. ^{17}O NMR-chemical shift calculated for various sized water clusters plotted against the apparent "coordination index", as defined in the text.

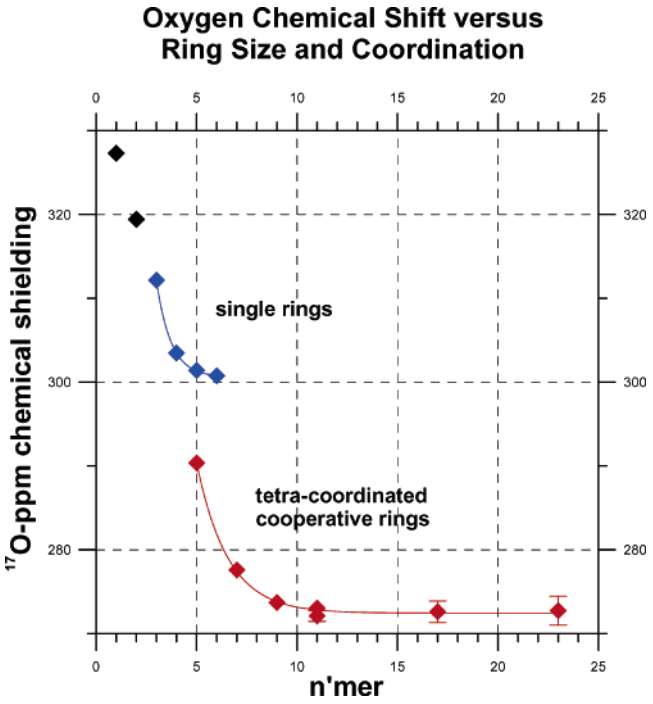

Figure 2. The effects of ring size and coordination, defined in terms of hydrogen bonding, on the chemical shielding tensor in water clusters. Reference values for the water monomer and dimer are shown in black; two-coordinated water molecules in single ring systems are shown in blue; and tetrahedrally four-coordinated waters in cooperative clusters are shown as red diamonds.

coordination index is merely an arbitrary construct so as to enable graphical display of the chemical shielding data in a comprehensible form. The digit after the decimal point does not have physical significance. The solid bars represent the range of values observed for the different oxygens and not individual values.

Figure 2 shows the effect of ring size and coordination on the chemical shielding tensor, with reference values for the water monomer and dimer given. Two-coordinated and four-coordinated water molecules yield asymptotic values for the ^{17}O-chemical shielding tensor of approximately 300 and 272 ppm, respectively.

The ^{17}O shifts are sensitive to ligand environment, that is, whether the water molecule acts as a single or double donor and/or acceptor. Moreover, lack of ring strain results in higher shifts than for systems in which the ligand environment is similar but part of a strained, typically three-membered ring. In the larger, more complex water clusters, the ^{17}O shifts fall into groups reflecting their electronic environment. (Detailed results with average values and standard errors are given in the form

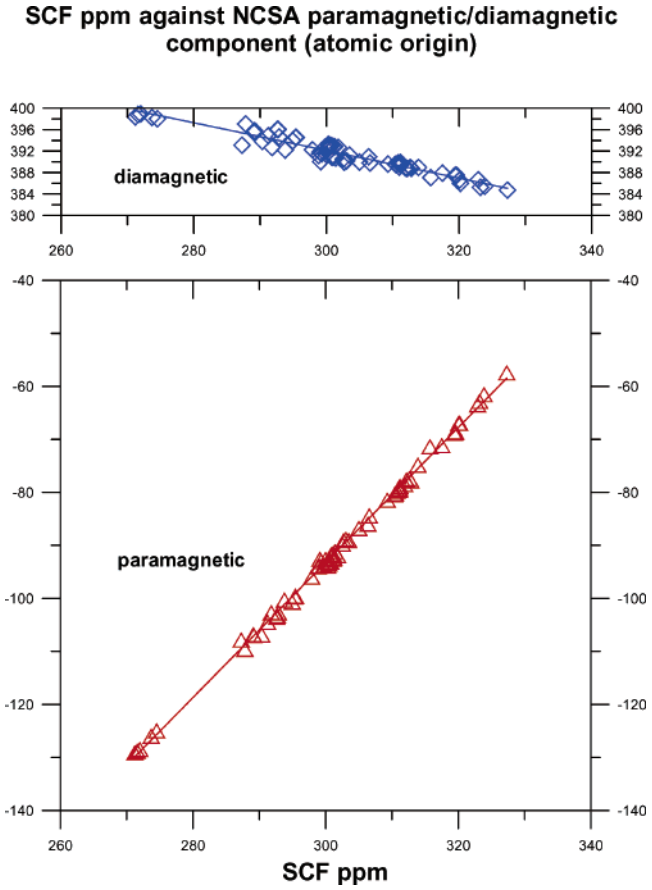

Figure 3. Separation of the diamagnetic and paramagnetic components of the ^{17}O-chemical shielding tensor as the magnitude of the tensor decreases with increasing hydrogen-bonding cooperativity and coordination. These results were obtained using MPW1PW91/6-311+G-(2d,p) GIAO calculations within the G03 program.

of tables in the Supporting Information available on request from the corresponding author at klein@institut.physiochem.uni-bonn.de.) ^{1}H-chemical shifts depend mainly on whether the hydrogen atom is involved as a hydrogen-bond donor, or not, with second-order effects due to cooperativity (defined as the presence of a sequence of water molecules linked regularly as both donor and acceptor in an alternating fashion). The abbreviations used, for example, 2A/2D, indicate the number of acceptor and donor "valencies" occupied for the water molecule in question.

Some generalizations may be drawn from the data in Figures 1 and 2. First, ^{17}O-chemical shifts increase as the number of hydrogen-bonding valencies are filled; second, cooperativity results in increased shifts especially in the interlinked ring systems; and third, the effects of ring size and hence relief of ring strain in causing an increase in chemical shift reach a plateau by $n = 5$. The water ^{17}O-chemical shielding tensor decreases as the ring size increases with values for the trimer, tetramer, pentamer, and hexamer of 312.1, 303.5, 301.4, and 300.8 ppm, respectively. Chemical shielding for water that is zero-, one-, two-, three-, or four-coordinated shows a progression from 327 ppm to near to 272 ppm, with considerable overlap between the groups. There appears to be a very large jump within the four-coordinated group from ~290 ppm to ~272 ppm on attaining a highly symmetric, cooperative structure with almost perfect tetrahedral symmetry for the hydrogen-bonded water molecules.

The chemical shielding tensor for ^{1}H that acts as a hydrogen-bond donor in a highly cooperative and symmetric environment

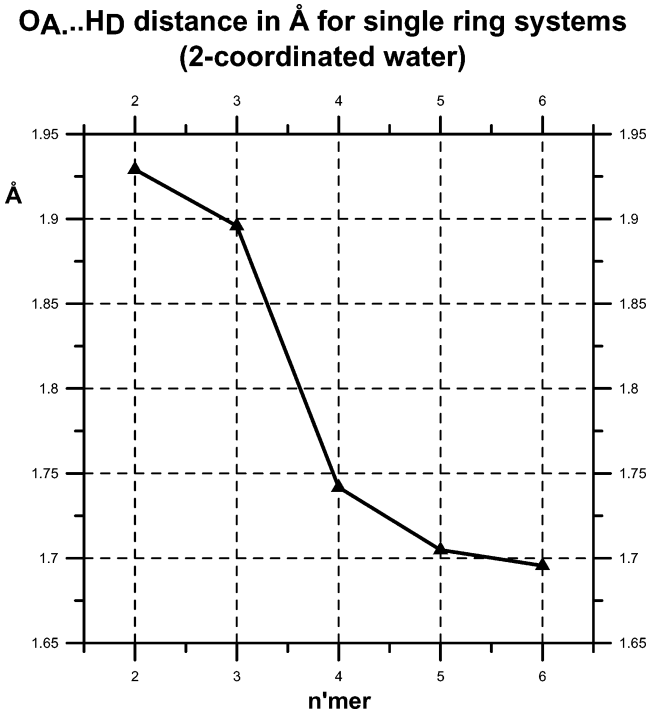

Figure 4. The effects of ring size on the $O_A\cdots H_D$ distance for hydrogen bonding between adjacent, two-coordinated water molecules in single, essentially planar ring systems ($n = 3-6$).

decreases to ~24 ppm as compared to an average value for a noninteracting hydrogen of 31.0−31.5 ppm, representing a calculated chemical shift of ~7 ppm.

In Figure 3, the calculated SCF (GIAO) chemical shift is plotted against the diamagnetic and paramagnetic components obtained by natural chemical shielding analysis (NCSA)[29] within the G03 program. The NCSA total shift and SCF chemical shift for ^{17}O are highly correlated ($R = 0.9973$), as would be expected, with the GIAO results being approximately 0.5−1.5 ppm larger (data not shown). The values for ^{1}H show differences in the first or second decimal place. It is clear from Figure 3 that as the ^{17}O-chemical shift increases, it is the paramagnetic component that is responsible for this offset by about 20% by the increasing diamagnetic shielding.

Electron Density Topological Analysis. Wave function files (6D 10F) were written for all minimized water clusters and then analyzed for electron density topology using the AIM2000[24] and Morphy98[25] programs. Average values for the electron density, $\rho(r)$, and its Laplacian, $\nabla^2\rho(r)$, at the (3,−1) bond critical point for the O···H hydrogen bonds are shown in the Supporting Information, which may be obtained on request from the corresponding author at klein@institut.physiochem.uni-bonn.de. We follow the standard (3,−1) topological notation used by Bader to indicate the bond critical point (BCP) as the point from which the electron density gradient becomes more negative along two mutually perpendicular axes orthogonal to the internuclear axis while rising in either direction along this axis; the BCP represents a saddle point with a maximum of electron density in two directions at right angles to the internuclear axis and a minimum along it.

Reflecting the changes in hydrogen-bond geometry, in which the donor−acceptor separation approaches an asymptotic value of ~1.70 Å (Figure 4), the electron density and its Laplacian at the bond critical point versus ring size in single ring systems, shown in Figure 5A and 5B, demonstrate effects similar to those of the ^{17}O-chemical shifts discussed above. Whereas the cyclic

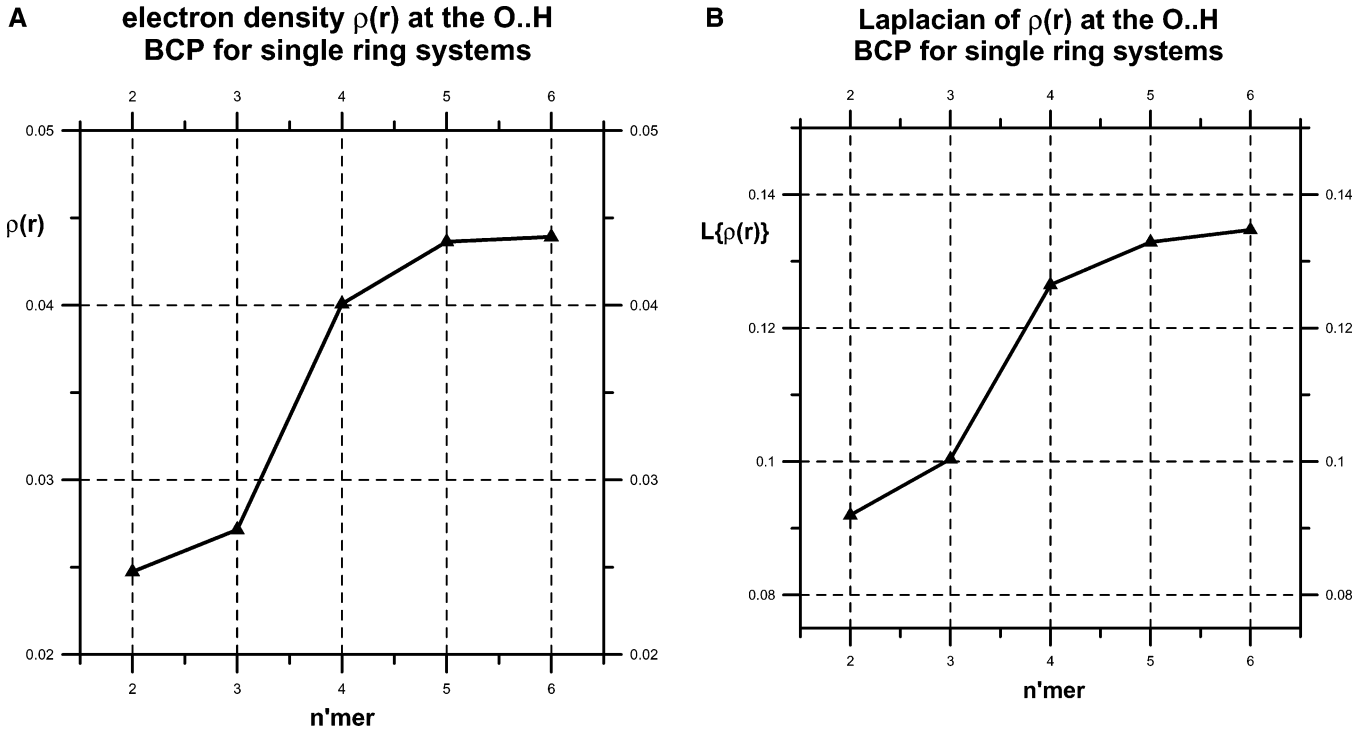

Figure 5. (A) The effects of ring size on the electron density $\rho(r)$ at the $O_A\cdots H_D$ bond critical point (BCP) for hydrogen bonding between adjacent, two-coordinated water molecules in single, essentially planar ring systems ($n = 3-6$). (B) The effects of ring size on the Laplacian of $\rho(r)$, $\nabla^2\rho(r)$, at the $O_A\cdots H_D$ bond critical point (BCP) for hydrogen bonding between adjacent, two-coordinated water molecules in single, essentially planar ring systems ($n = 3-6$).

trimer differs very little from the dimer − $\rho(r) = 0.02715$ au as compared to 0.02474 au − the electron density increases for the cyclic tetramer (0.04008 au) and reaches an apparent asymptote by the cyclic pentamer or hexamer, 0.04313 and 0.04392 au, respectively. This is also paralleled by the Laplacian of $\rho(r)$ which determines whether electronic charge is locally concentrated, that is, $\nabla^2\rho(r) < 0$, or depleted, that is, $\nabla^2\rho(r) > 0$. Similar results have been found for two rings fused through a single, four-coordinated water molecule (see below). More remarkable, however, is that the incorporation of the cooperative ring pentamer into larger structures such as the undecamer (5^3), the heptadecamer (5^6), and the tricosamer (5^9) (this terminology means that there are nine pentagons present) with extended cooperativity throughout the ring system does not result in any significant change in electron densities at the BCPs, possibly even a slight diminution. Another notable feature of these systems is that the $\rho(r)$ values average out to within approximately ±2% even though the water molecules are not all equivalent − for example, in the undecamer, heptadecamer, or tricosamer, the "internal" waters are tetracoordinated, whereas the "outer" waters act as single donors and acceptors, albeit cooperatively. The strained three-ring ("cyclopropane" type) systems, that is, the cyclic trimer, the bicyclic or twisted pentamer, and the tridecamer, all have similar values for $\rho(r)$ and its Laplacian $\nabla^2\rho(r)$ of around 0.027 and 0.10 au, respectively.

Full AIM electrostatic multipole analysis for all of the atoms in these single ring systems and including the water dimer for reference ($n = 2-6$) provides a measure of the extent of charge transfer for both the hydrogen and the oxygen atoms involved in hydrogen bonding. These data are shown in Figure 6A. The asymptotic values for hydrogen and oxygen, respectively, of +0.82 and −0.88 au are not quite equal. This is not an error because, although the complete system is obviously electroneutral and there is no artifactual "loss of charge" during the calculation, there are small induced changes observed affecting the nonbonding hydrogens that are at least an order of magnitude smaller (∼ +0.06 au).

Natural Bond Orbital (NBO) Analysis. An NBO file was written for each minimized water cluster and then analyzed using a stand-alone version of NBO 5.0[20] with the option E2PERT set to 0.10 kcal/mol. The changes in antibonding σ^* O−H orbital occupancies are shown in Figure 6B for the hydroxyl group providing the hydrogen-bond donor ($O-H_D$), or not involved in bonding but nonetheless attached to an oxygen acceptor (O_A-H). Cooperative hydrogen bonding results in an increase in antibonding orbital occupancy for the $O-H_D$ group of between 50- and 100-fold as compared to the nonbonded OH.

As before, the σ^* antibonding orbital occupancy shows a clear effect with ring size, increasing from a value for the dimer of 0.015 to 0.019 for the strained cyclic trimer, through 0.038 for the cyclic tetramer to a constant value of between 0.041 and 0.042 for the pentamer, hexamer, undecamer, heptadecamer, and tricosamer (the data for the latter three clusters are not shown). The values for the cyclic pentamer are the same within experimental error as those for the fused *n*-pentamers. Unlike the electron density, there appears to be a slight increase in occupancy of the order of ∼5−10% in the strained three-ring series, that is, the cyclic trimer, twisted pentamer, and tridecamer.

Two-Ring Systems Fused at a Four-Coordinated Water. In a series of hydrogen-bonded water clusters consisting of two rings fused at a central, four-coordinated water molecule linking two-coordinated water molecules, that is, $[2n - 1]$ clusters each containing two *n*-rings (see Scheme 2), both the electron density, $\rho(r)$, at the hydrogen-bond BCP and its Laplacian, $\nabla^2\rho(r)$, increase with ring size, as shown in Figure 7. Again, we find

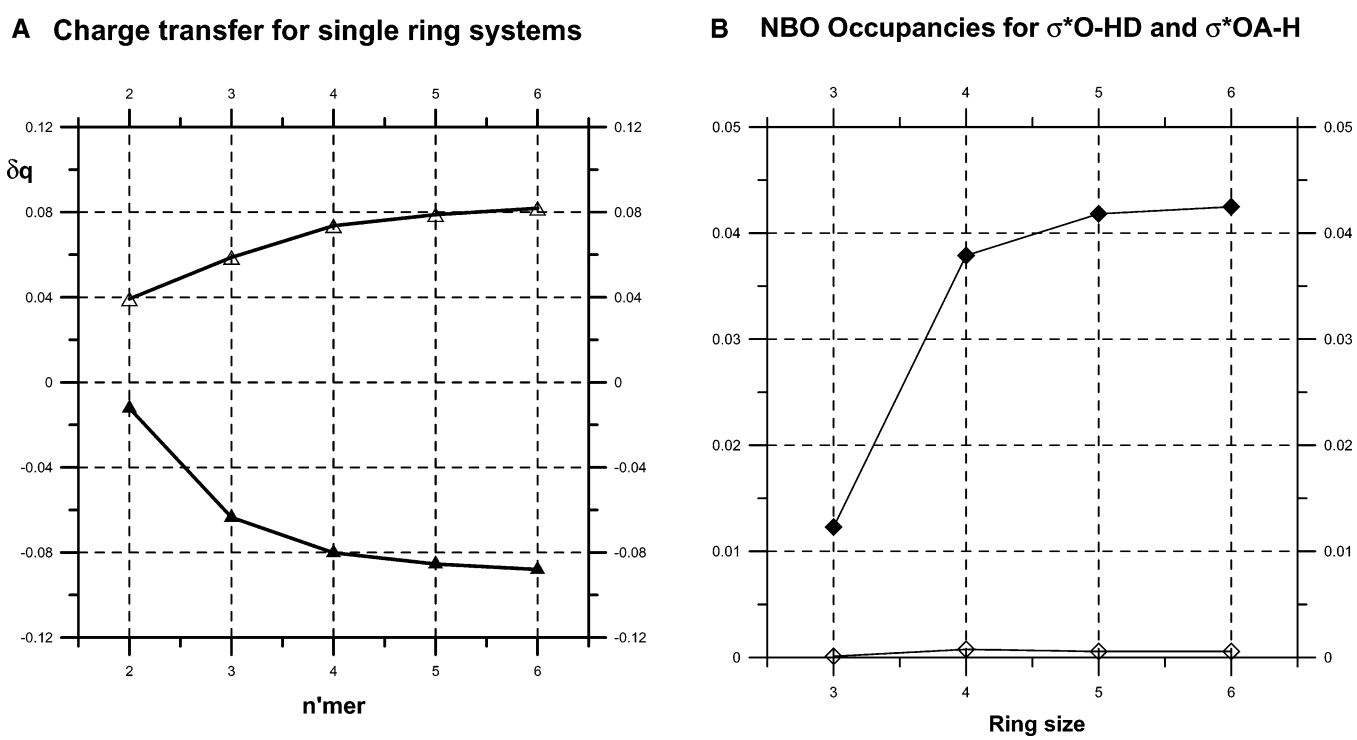

Figure 6. (A) The effects of ring size on charge transfer, calculated by atom basin integration of the hydrogen (△) and oxygen atoms (▲), for hydrogen bonding between adjacent, two-coordinated water molecules in single, essentially planar ring systems ($n = 3-6$). The water monomer was used as the reference structure for the monopole electrostatic moments (= "charge"). (B) The effects of ring size on NBO antibonding orbital occupancies for hydrogen bonding between adjacent, two-coordinated water molecules in single, essentially planar ring systems ($n = 3-6$). Occupancies are shown for the σ*O−HD (◆) and σ*OA−H (◇) antibonding orbitals. The σ*OA−H antibonding orbital serves as an internal reference as this O−H group does not participate in a hydrogen bond.

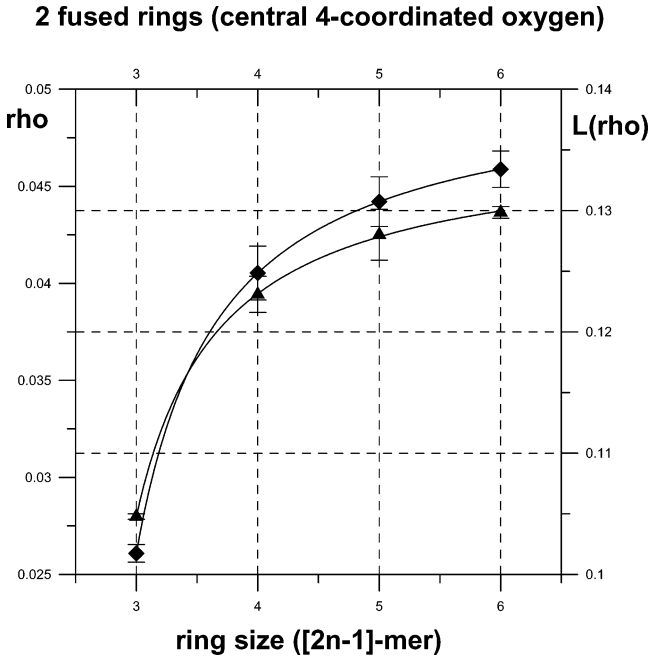

Figure 7. The effects of ring on the BCP electron density and its Laplacian in systems containing two equal rings ($n = 3-6$), fused at a central four-coordinated water molecule to give a [$2n - 1$]-mer ($m = 5, 7, 9, 11$). The electron density (▲) and its Laplacian (◆) are shown.

that the changes in electron density and its Laplacian are averaged out over the ring systems.

The chemical shielding tensor for a four-coordinated water oxygen in these two-ring fused systems is markedly dependent on geometry as shown in Figure 8A. The chemical shielding tensor for ^{17}O drops from ∼292 ppm to an asymptote around ∼272 ppm as the ring size increases from three to six. A similar effect is seen for the chemical shielding of the two-coordinated oxygen atoms, with a drop from ∼311 to ∼300 ppm. The difference between oxygen atoms in five- and six-membered rings is small, probably within the error of the calculation.

The chemical shielding anisotropy (CSA)[30] for ^{17}O decreases with improved tetrahedral coordination as shown in Figure 8B. These data include not only the two-ring fused systems but also all of the edge-fused pentagonal structures studied. The CSA value for a single tetrahedrally coordinated water molecule without the effects of donor−acceptor cooperativity, containing a so-called "naked" tetrahedral oxygen, is shown by the horizontal dotted line.

Atomic Basin Integration, Multipole Electrostatic Analysis, and the Electric Field Gradient. To analyze the results further, we introduce here a multipole analysis of the electron density[31] for which we give the main mathematical formula below.

The electrostatic potential induced at a distance r by a charge distribution which can be expanded in multipole terms is given by

$$\Phi(r) = \frac{1}{4\pi\epsilon_0}\left\{\frac{q}{r} + \frac{\mu\cos\theta}{r^2} + \frac{\Theta(3\cos^2\theta - 1)}{2r^3} + ...\right\} \quad (1)$$

whereas the electrostatic interaction, $\psi_{q,q'}$, between two charge

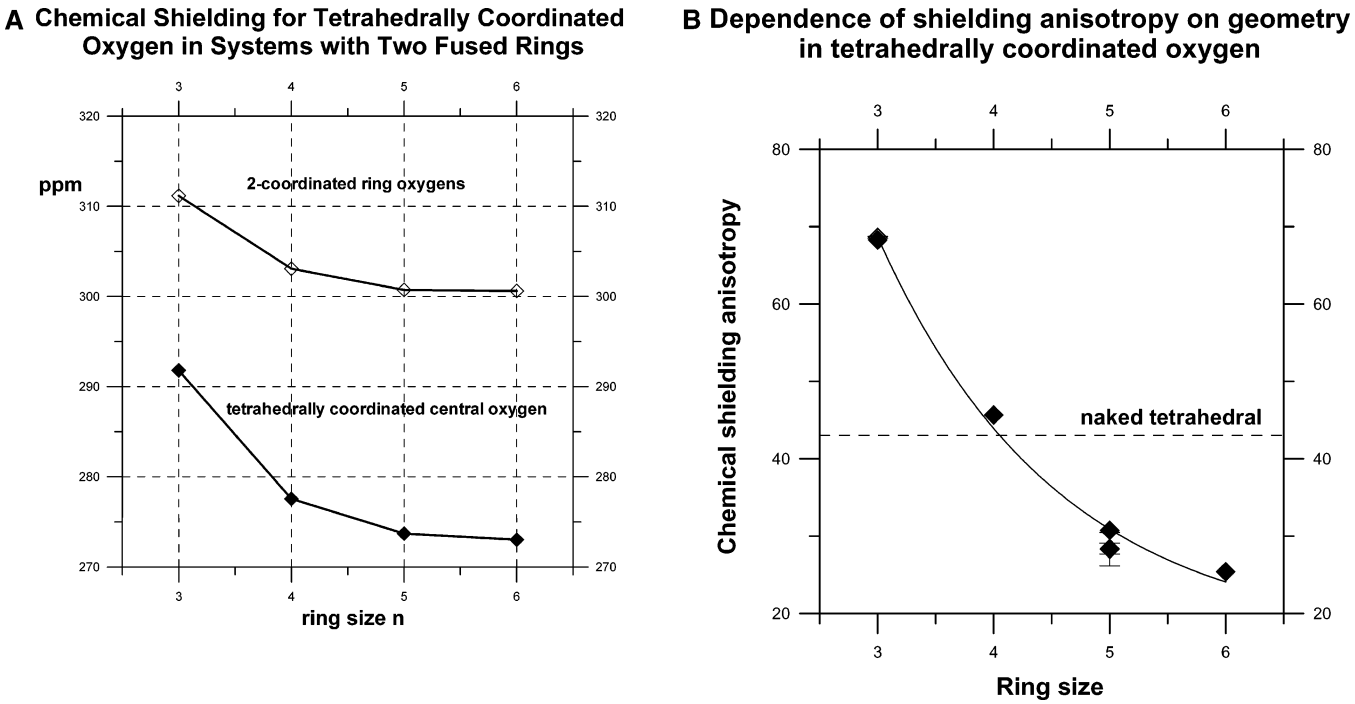

Figure 8. (A) The effects of ring size on the chemical shielding for two-coordinated and tetrahedrally four-coordinated ^{17}O in systems containing two equal fused rings (Scheme 2: $n = 3, 4, 5, 6$; $m = 5, 7, 9, 11$). The two-coordinated (◇) and the four-coordinated (◆) oxygens are shown. (B) The dependence of the ^{17}O-chemical shielding anisotropy on geometry for tetrahedrally coordinated oxygen. Ring size is plotted against the shielding anisotropy (defined as $\sigma_{zz} - (\sigma_{xx} + \sigma_{yy})/2$). The horizontal dotted line indicates the value of the chemical shielding anisotropy for a naked tetrahedrally coordinated water molecule, that is, one not involved in a cooperative ring system (structure 5T).

systems is

$$\psi_{q,q'} = \begin{Bmatrix} \frac{qq'}{r} \\ +\frac{\mu\mu'}{r^2}(q\mu' \cos\theta + q'\mu \cos\theta') \\ +\frac{1}{2r^3}(q\Theta'(3\cos^2\theta' - 1) + q'\Theta(3\cos^2\theta - 1)) \\ \frac{3}{2r^4}\begin{pmatrix} \mu\Theta'\{\cos\theta(3\cos^2\theta' - 1) + 2\sin\theta\sin\theta'\cos\theta'\cos\zeta\} \\ +\mu'\Theta\{\cos\theta'(3\cos^2\theta - 1) + 2\sin\theta'\sin\theta\cos\theta\cos\zeta\} \end{pmatrix} \\ +\frac{3\Theta\Theta'}{4r^5}\begin{pmatrix} 1 - 5\cos^2\theta - 5\cos^2\theta' + 17\cos^2\theta\cos^2\theta' \\ +2\sin^2\theta\sin^2\theta'\cos^2\zeta + 16\sin\theta\sin\theta'\cos\theta\cos\theta'\cos\zeta \end{pmatrix} \\ + \ldots\ldots \end{Bmatrix} \quad (2)$$

The quadrupole is commonly defined as follows:

$$\Theta = \frac{1}{2}\begin{pmatrix} \sum_i q_i(3x_i^2 - r_i^2) & 3\sum_i q_i x_i y_i & 3\sum_i q_i x_i z_i \\ 3\sum_i q_i x_i z_i & \sum_i q_i(3y_i^2 - r_i^2) & 3\sum_i q_i y_i z_i \\ 3\sum_i q_i x_i z_i & 3\sum_i q_i y_i z_i & \sum_i q_i(3z_i^2 - r_i^2) \end{pmatrix} \quad (3)$$

Quadrupoles are usually reported in terms of the principal axes, so that the off-diagonal elements are zero.

$$\Theta = \begin{pmatrix} \Theta_{\alpha\alpha} & 0 & 0 \\ 0 & \Theta_{\beta\beta} & 0 \\ 0 & 0 & \Theta_{\gamma\gamma} \end{pmatrix} \quad (4)$$

This definition enables one to assess the deviation from spherically symmetric charge distribution. In general, the interaction energy between two multipoles of order m and n decreases as $r^{-(m+n+1)}$. In the completely spherically symmetric case, this will reduce to

$$\Theta = \frac{1}{3}\sum_i q_i r_i^2 \quad (5)$$

The assignment of point charges centered on the atomic nuclei, although computationally convenient, assumes that the distribution of electrons around the nucleus is spherically symmetric; this is far from the case for the valence electrons in molecules containing either lone pair electrons or aromatic π-cloud systems. Wiberg and Rablen[32] found, using Bader's AIM method for partitioning the electrons in a molecule,[33] that the atomic charges obtained, that is, the monopole or zeroth order terms of the electrostatic multipole expansions, were substantially independent of the basis set used and gave good agreement with the experimental values for the methane and acetylene C−H bond dipoles, which other methods did not, providing generally more reliable values for organic molecules as compared to other partitioning procedures. As pointed out previously, however, the higher order moments are basis-set dependent and require a high level of theory before becoming stable. The distributed multipole model[34] accounts automatically for nonspherical, anisotropic effects brought about by lone pair electrons or π electrons. The highest multipole moment in the local Taylor expansion depends on the basis set used, with no multipole

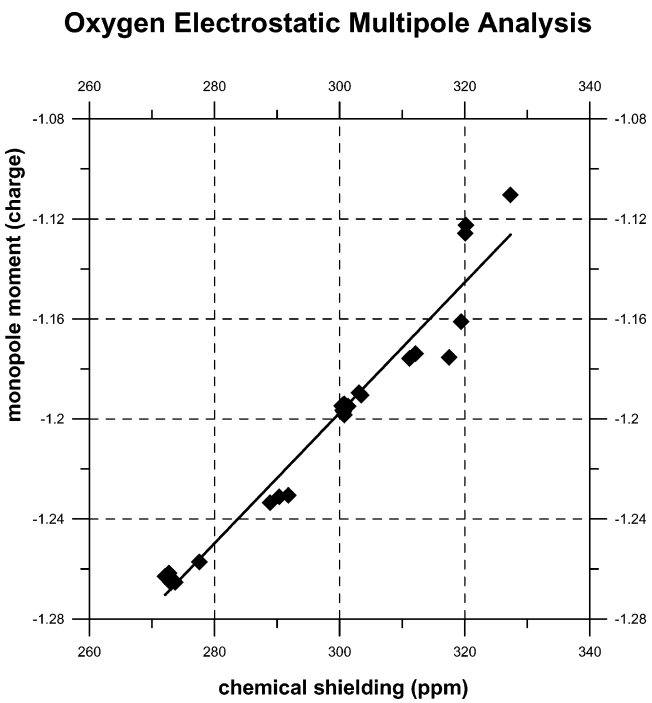

Figure 9. The dependence of the ^{17}O-chemical shielding tensor on the monopole electrostatic moment ("charge") for the range of water clusters studied, obtained by atomic basin integration using the Morphy98 AIM implementation as described in the text. The correlation coefficient, R^2, is 0.9507 with a residual mean squared deviation, $\hat{s}^2$, of 1.06×10^{-4}.

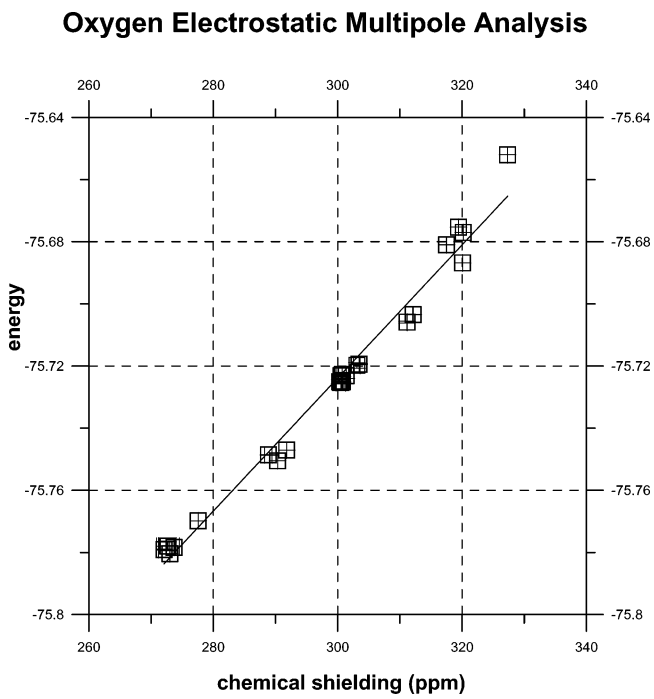

Figure 10. The relationship between the ^{17}O-chemical shielding tensor and the virial-corrected energy for the oxygen nucleus in the series of clusters studied, obtained as in Figure 9. The correlation coefficient, R^2, is 0.9829 with a residual mean squared deviation, $\hat{s}^2$, of 2.41×10^{-5}.

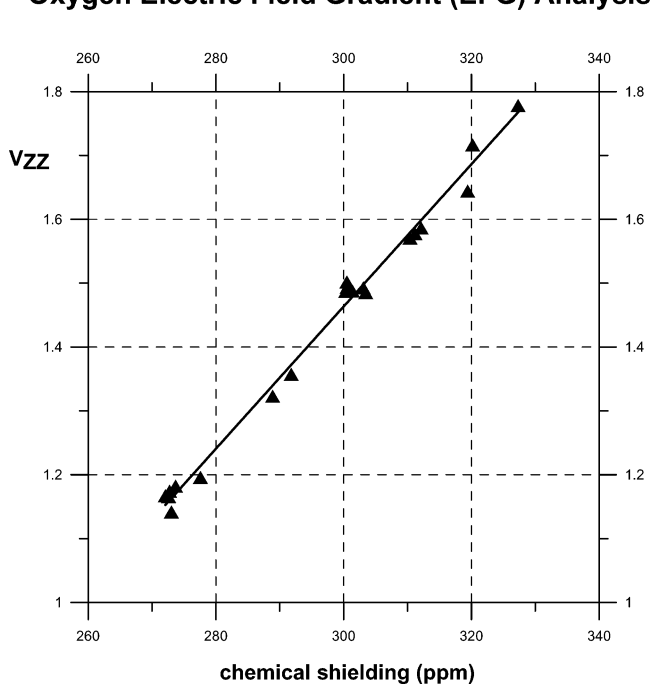

Figure 11. The relationship between the ^{17}O-chemical shielding tensor and the V_{zz} component of the electric field gradient (EFG), calculated at the MPW1PW91/6-311+G(2d,p) level. The correlation coefficient, R^2, is 0.9897 with a residual mean squared deviation, $\hat{s}^2$, of 3.78×10^{-4}.

moment higher than the sum of the angular quantum numbers being possible. The use of the most appropriate method for proportioning electronic charge is not trivial, as evidenced by the discussion recently in a paper by Guerra et al.[35] These authors claim that the Voronoi deformation density (VDD) and Hirschfeld schemes give similar and "chemically meaningful" results, whereas both the Bader and the natural population analysis (NPA) methods overestimate ionic character giving values that were too extreme. The Mulliken method was again judged to be quite useless, in line with other comments in the literature, due to pronounced basis-set dependence. In using Bader's AIM analysis in this paper, and taking into account Guerra et al.'s comments, we concentrate not on absolute atomic charge (actually the monopole moment) but on incremental changes from the value for the water monomer. Popelier's MORPHY98 program,[25] used here for the analysis of the wave function, provides electrostatic moments as $(2l + 1)$ components plus the magnitude in atomic units, that is, multiplied by $-e$, the fundamental unit of electron charge.

As can be seen from Figures 9−11, the changes in the chemical shielding tensor for oxygen-17 associated with changes in the coordination and geometry of hydrogen bonding for the water molecule are well correlated with its electrostatic monopole moment, that is, the "charge", the virial-corrected energy (indicating stabilization), and the V_{zz} component of the electric field gradient (EFG). Other components of the electrostatic multipole analysis were less well correlated with changes in the chemical shielding tensor, in particular, the dipole and hexadecapole moments, although the quadrupole and octapole moments as well as the atomic volume showed reproducible trends. For example, the atomic volume, vol(Ω), defined as the volume out to the $\rho(r) = 0.001$ au contour, showed a decrease of approximately 15−20% corresponding to wave function contraction as the chemical shielding tensor decreased and the strength of the hydrogen bonding increased. Hydrogen-bonded hydrogen atoms, on the other hand, showed marked contraction of their atomic volumes as compared to non-hydrogen-bonded hydrogens, amounting to a nearly 50% reduction. Decreases in the ^{17}O-chemical shielding tensor are strongly correlated with a decrease in the V_{zz} component of the EFG. With a reduction

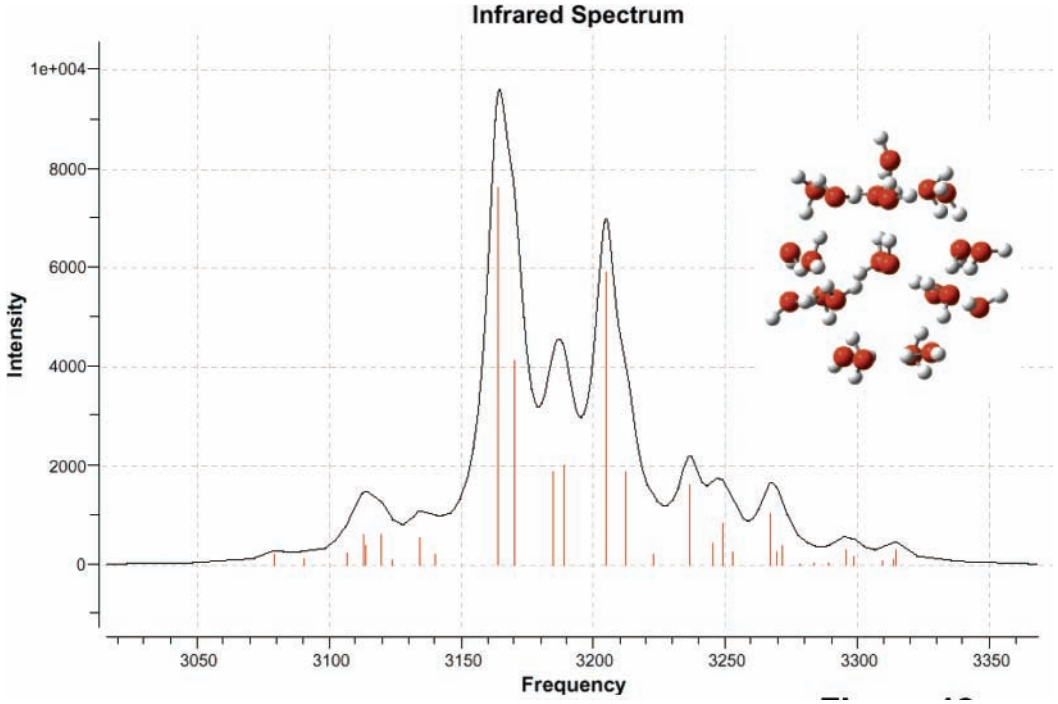

Figure 12. Infrared spectrum for the tricosamer $(H_2O)_{23}$, geometry minimized and calculated at the MPW1PW91/6-311+G(2d,p) level using the option scf=tight. The region of the O−H stretching vibrations is shown as frequency in wavenumbers (corrected for scaling) against intensity. The estimated scaling factor at this level of theory is 0.9429, as discussed in the text.

in V_{zz}, there is a relatively poorly correlated increase or trend in the calculated asymmetry parameter (data not shown) from 0.79 for the water monomer to $\sim 0.93 \pm 0.03$ for tetrahedrally four-coordinated oxygen in the larger clusters, comparable to ice Ih.[36] The asymmetry parameter for two-coordinated oxygen is ~3% less than that for four-coordinated oxygen, and ring strain, as seen with a ring size $n = 3$, reduces both by another ~3−5%. Ring strain also results in higher values for V_{zz} by ~10−15%, if one compares either two- or four-coordinated water molecules in three rings with larger ring systems.

Synchronization of the IR OH-Stretching Vibrations. Highly cooperative systems in which water molecules are hydrogen-bonded through alternate donor−acceptor ligands are characterized by synchronization of the water OH-stretching vibrations in the infrared spectrum, clearly seen in the case of hydrated glucopyranose.[22] We have also observed this behavior in the water clusters studied in this paper. For example, the tricosamer $(H_2O)_{23}$, containing nine interlocking pentagonal water rings, yields an IR spectrum calculated at the MPW1PW91/6-311+G(2d,p) level showing a complex pattern of synchronization involving both symmetric and asymmetric O−H stretching modes; there are no imaginary frequencies observed for this geometry, thus indicating a true minimum and not a transition state. This synchronization, or phase-locking, affects to a greater or lesser extent all of the water molecules in the cluster, a truly cooperative effect.

The wavenumbers for the most intense vibrations in the spectrum for the tricosamer cluster, after correction for scaling (scaling factor = 0.9429),[22,23] are as follows, shown with their relative intensities in brackets: 3164 cm^{-1} (1.0); 3170 cm^{-1} (0.54); 3185 cm^{-1} (0.24); 3189 cm^{-1} (0.26); 3205 cm^{-1} (0.77); 3213 cm^{-1} (0.24); and 3237 cm^{-1} (0.21). The O−H stretching region of the IR spectrum is shown in Figure 12. This partial spectrum, characterized by multiplets including two major peaks centered at approximately 3165 and 3205 cm^{-1}, should be compared with the much simpler one for the water monomer in the gas phase consisting of asymmetric (3756 cm^{-1}) and symmetric stretching modes (3657 cm^{-1}). The red-shifts as compared to the water monomer are substantially greater than those for hydrated glucopyranose reported by us previously.[22]

Polarizable Continuum Model (PCM) Calculations. For the continuum description of the solvent, we used the Integral Equation Formalism (IEF).[37] In this approach, the solute is represented as a quantum mechanical charge distribution inside a cavity of molecular shape immersed in a macroscopic dielectric with known permittivity ϵ. The electrostatic interactions between solute and solvent can then be represented in terms of an apparent surface charge on the cavity, which produces a perturbation to the solute wave function, translated as an operator to be added to the solute Hamiltonian. The solution of the resulting quantum mechanical problem gives the solute wave function modified by the solvent in a mutually polarized way. IEFPCM has been generalized to the GIAO method so as to include solvent perturbation operators in the response scheme required to compute the nuclear shielding; for more details on the formalism, see ref 38. In the IEFPCM model, the molecular cavity is obtained in terms of interlocking spheres centered on the nuclei. The chosen radii are here 1.52 Å for oxygen and 1.2 Å for hydrogen (all of the radii are then multiplied by a factor equal to 1.2 to take into account the fact that atomic bonds or lone-pair centers of the solvent molecules are normally located farther from the solute atoms than the van der Waals radius).

The IEFPCM model has been applied here both to the single water molecule (the monomer) and to clusters of increasing dimensions (from dimer to pentamer). IEFPCM calculations of oxygen nuclear shieldings are shown in Figure 13 as differences with respect to the gas-phase monomer value. Two sets of data are given referring to gas-phase geometries (IEFPCM(gvac)) and to geometries which have been reoptimized in solution at the MP1PW91/6-311+G(2d,p) level (IEFPCM), exactly as for the nonsolvated gas-phase values.

The results for the chemical shift of oxygen in the monomer disagree with experiment not only in absolute value but also in

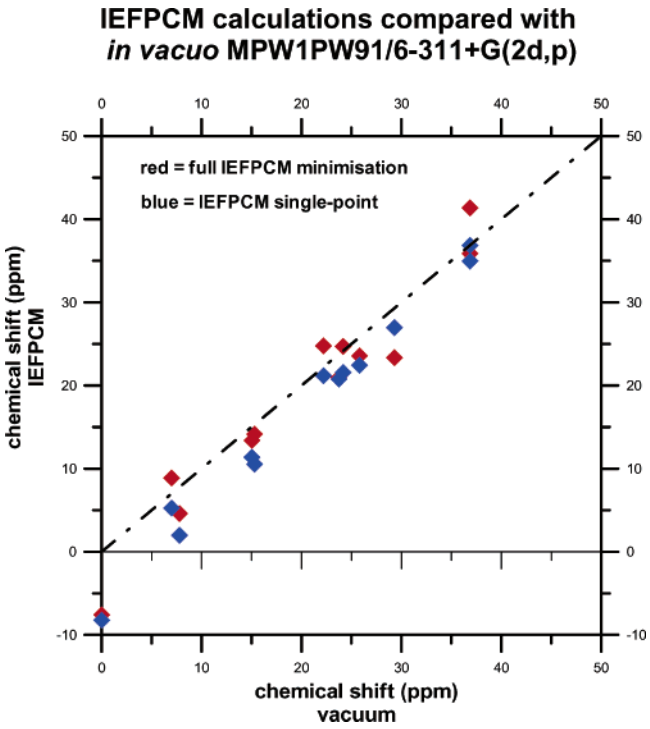

Figure 13. Polarizable continuum model (IEFPCM) calculations of the ^{17}O-chemical shift for a series of water clusters from $N = 1$ to $N = 5$ at the MPW1PW91/6-311+G(2d,p) level of theory using Gaussian 03. The chemical shift calculated without using the IEFPCM method (*x*-axis) is shown against the results obtained using the IEFPCM method (*y*-axis). Cluster geometry was minimized either in vacuo (blue) or with IEFPCM solvation corrections (red), followed by calculation of the chemical shifts using IEFPCM. The dotted and dashed line at 45° represents absolute equality between the two sets of chemical shifts.

direction (sign) − see the points on the *y*-axis of the graph at 0 ppm. The computed gas-to-liquid shift is around −8 ppm, while the experimental value is +36 ppm. The same trend has been observed in previous calculations using other continuum models as well as the RISM-SCF approach.[39] The two parallel sets of data (IEFPCM and IEFPCM(gvac)) also clearly show that the wrong description is not due to an effect of the molecular geometry. Also, the "solute" water molecule, optimized in the liquid phase, in fact predicts a negative shift.

With clusters (and thus explicitly with inclusion of short-range H-bonding effects), the use of the polarizable continuum model produces little systematic effect on the calculated ^{17}O shielding tensor. Only in the case of the dimer does the use of IEFPCM actually reduce the apparent chemical shielding by a substantial amount (40% and 75%) as compared to the value for the same cluster in the gas phase. In all other cases, that is, other than for the monomer and dimer, this effect is within ±20% of the gas-phase value as shown in Figure 13. The effects on the gas-phase or solvated geometries are not important for either the monomer or the larger clusters.

One must conclude that SCRF methods such as IEFPCM cannot be used to model adequately solvation effects on the ^{17}O nuclear shielding for liquid water. The analysis required, however, is more complex than that for other hydrogen-bonded solute−solvent systems. In fact, in these other systems, it is evident that a continuum-only description cannot model strong first-shell hydrogen-bonding effects, giving a computed shift which accounts for only a part of the observed effect, but which still goes in the correct direction. By contrast, for liquid water, the continuum model used alone produces an effect that is the opposite of that observed. It thus seems that the complex and highly ordered environment that each water molecule experiences in the liquid phase has an effect on the oxygen nuclear shielding which can be only realized in terms of explicit QM clusters. This suggests that the chemical shift of oxygen is extremely sensitive to subtle details of the intermolecular interaction and in particular to the exchange or overlap of electrons between solute and solvent.

Summary and Conclusions

This paper represents the first reported extensive analysis of the ^{17}O NMR-chemical shielding tensor behavior of water molecules embedded in large clusters that takes account explicitly of hydrogen-bond geometry and cooperativity as evidenced by the electron density topology of the hydrogen bonds, charge transfer for the donor and acceptor atoms, NBO antibonding orbital occupancies, electric field gradients, and a full electrostatic multipole analysis for the oxygen and hydrogen atoms involved.

The full range of changes in the ^{17}O-chemical shielding tensor corresponding to an experimental value of ∼49 ppm for the phase change from water vapor at 100 °C to ice at 0 °C can be calculated quantum mechanically by taking into account explicitly cluster geometry and donor−acceptor cooperativity. Cooperativity in water clusters is manifested by increases in chemical shift, reduction in donor−acceptor distances, greater linearity in the O···H−O angle, increased charge transfer and donor−acceptor interaction energies, increases in the electron density and its Laplacian at the hydrogen-bond bond critical point (BCP), increased O−H antibonding orbital occupancies, together with a reduction in the V_{zz} component of the electric field gradient, as well as changes in electrostatic multipole moments and a marked synchronization of infrared OH stretching vibrations with substantial red-shifts, similar to data reported recently for hydrated glucopyranose.[22]

As might be expected intuitively on the basis of geometrical considerations, hydrogen bonding in single two-coordinated rings is most effective as the cluster size reaches five or six water molecules as evidenced by the values for the donor−acceptor O···H distance, the electron density at the hydrogen-bond BCP, the Laplacian of the electron density, charge transfer on the donor hydrogen and acceptor oxygen atoms, the NBO antibonding orbital occupancies, and the ^{17}O NMR-chemical shielding tensor, all reaching asymptotic values as shown in Figures 1, 2, and 4−8. In systems containing two rings fused at a central four-coordinated water molecule (Schemes 1 and 2: structures 5Tw, $n = 5$, 7, 9, and 11), the properties of both the two-coordinated water oxygens and the four-coordinated water oxygens also show this asymptotic behavior as the ring size reaches five or six. In particular, the chemical shielding tensor for the two-coordinated and four-coordinated oxygen atoms approaches an asymptotic value of ∼300 and ∼272 ppm, respectively. It is not difficult to understand why the four-coordinated oxygen atom in the fused ring nonamer or undecamer should be in an almost ideal geometric and stable electronic environment, because the four hydrogen-bond ligands in this situation, two donors and two acceptors, are arranged with almost perfect tetrahedral symmetry. The virial-corrected energy of the oxygen atom decreases in line with the decrease in the chemical shielding tensor and electric field gradient (Figures 9 and 11), indicating increasing stabilization as the geometry improves.

Large water clusters consisting of multiple interlocking cooperative five-membered rings, such as the undecamer ($n = 11$), heptadecamer ($n = 17$), or tricosamer ($n = 23$), with an

increasing number of four-coordinated central water molecules, do not result in any marked increase in the ^{17}O-chemical shielding tensor. It seems that for a water oxygen atom to have a chemical shielding tensor close to 272 ppm, all that is required is that the water molecule is four-coordinated with a geometry close to tetrahedral symmetry, that is, with the angle between adjacent ligands close to 109°, in at least a two-ring system showing donor−acceptor cooperativity. It is worth noting that the water oxygen atoms in the two clathrate-type cage structures studied (Zottola and Klein to be published), the 5^{12} eicosamer and the $5^{12}6^2$ tetracosamer, show shielding tensors in the range ∼294−296 ppm because the water molecules are only three-coordinated despite being embedded in a highly cooperative fused five-ring system.

Our approach using explicit ab initio calculation of NMR chemical shifts for ^{17}O in water clusters of well-defined ligand geometry and cooperativity can be used to provide, in principle at least, a chemical shielding or shift scale indicating the average coordination number for solvent water under various conditions. It should be pointed out that Car-Parrinello QM/MM methods provide similar results by considering the time-averaged environment of the water molecules implicitly. We have shown in the current paper that taking a single water molecule from the monomer state in the gas phase to a highly ordered cluster in which the water acts as both a donor and an acceptor for four hydrogen bonds in total results in a reduction of the ^{17}O NMR-chemical shielding tensor, that is, a chemical shift, of ∼55 ppm. In comparing this value with the experimental value, it should be pointed out that water molecules at 100 °C on the point of changing from vapor to the liquid state cannot be considered completely isolated from one another with absolutely no hydrogen bonding and, in addition, ice at 0 °C will not be completely ordered, that is, with exactly four hydrogen-bond ligands on average per water molecule.[40] Also, given the proviso that our calculated value of ∼55 ppm is unlikely to be extremely precise, this still means that our result would indicate a change of the average hydrogen bonding per water molecule on going from the gas to ice phase of ∼3.5. This is probably not unreasonable as a crude estimate. Moreover, a similar argument would suggest that this is made up, again on average, of a change of ∼2.6 hydrogen bonds for the transition from the gas to liquid phase at 100 °C, followed by ∼0.3 for liquid water on going from 100 to 0 °C, and a final ∼0.6 for the liquid-to-ice phase transition. Similar approximate figures are obtained by considering the latent heats of fusion or vaporization, as well as the heat capacity, for water together with the best known interaction energy for the water dimer of 5.0 kcal/mol[41] representing one hydrogen bond. Such estimates are in keeping with what is known from NMR studies and MD simulations for liquid water.[42]

We have shown in a previous publication[43] that certain diols, containing a terminal methyl-carbinol group (CH_3CHOH), are able to cause a downfield shift in the ^{17}O NMR-chemical shielding of water molecules, which we interpreted as structuring of the water molecules in the vicinity of the methyl group. The maximum downfield shift observed in these binary glycol−water systems was approximately 1.0−1.2 ppm, corresponding to "cooling" all of the water molecules on average by 25−30 °C. On the basis of the calculations reported in the present paper, such downfield shifts can be ascribed to an increase in the apparent average coordination of all of the individual water molecules by about ∼0.1, but representing a much greater change for just those water molecules directly involved in the interaction, averaged over the NMR time scale, resulting in an increase in the transfer of negative charge, increased stabilization of the oxygen atom, and a decrease in the electric field gradient experienced by the oxygen atom.

There is clearly a need to develop a model of the water molecule for use in molecular-mechanics (MM) force-fields that takes account of the phenomena highlighted in the present work, in particular charge transfer and cooperativity effects. Current models used in MM force-fields include potential functions, for example, SPC/E, ST2, TIP3P, TIP4P, and TIP5P, in which the water molecule is polarized by the inclusion of partial charges either on the hydrogen and oxygen atoms or on the bisector.[44] Specifically, any refined model for water must include terms for the degree of coordination, the distance and geometry of the O···H donor−acceptor pairs, charge transfer effects and cooperativity, and any structuring of the water layer close to the surface of a solute, such as a carbohydrate or protein, especially in the presence of fixed charge. Some form of switching function sensitive to the local H_2O molecular environment will be required to modulate the partial charges carried by the hydrogens and oxygen atom, in combination with an algorithm for determining the nature of the interactive environment for individual water molecules. This will, based on our current work, almost certainly need explicit consideration of solvent water out to the second hydration layer for individual water molecules if these effects are to be modeled accurately.

Consideration of solvent water as a simple continuum with average properties is, at very best, only a crude approximation in situations where appreciable interactions occur between monomers with effects, including charge transfer, which depend on their electronic environment. Indeed, the failure of continuum models, also in the form of their most recent implementations as used in the current study, in describing the changes in the ^{17}O-chemical shielding tensor for water on passing from the vapor to the liquid phase now presents a clearer picture. The quantitative analysis we have performed in terms of cooperativity effects shows that the changes are determined essentially by the phenomenon of charge transfer between hydrogen-bonded water molecules in a well-defined geometrical environment. This three-dimensional cooperative effect cannot be simulated by an averaged (or mean) field as stipulated in the continuum model, which can only mimic the polarization effects. The latter is not only insufficient to describe the observed gas-to-liquid change in chemical shielding correctly but also leads to an incorrect answer in both magnitude and absolute sign (the computed gas-to-liquid shift using IEFPCM is around −8 ppm instead of the experimental value of +36 ppm).

In conclusion, it has to be noted that the accurate description of the ^{17}O-chemical shielding in liquid water is a quite unique problem as the quasi-structured arrangement which surrounds each water molecule and which is associated with cooperativity effects such as charge transfer is specific for this liquid phase alone; continuum solvation models have, in fact, been shown to be very effective in determining solvent effects on many molecular properties including nuclear shielding for a large number of solutes in very different solvents.[45]

Acknowledgment. R.A.K. would like to thank the Deutsche Forschungsgemeinschaft for financial support in the form of a project grant within the research program SFB 284/A1 during the initial stages of this work, and also the John von Neumann Institute for Computing, Forschungszentrum, Jülich, for the allocation of computational facilities. B.M. and J.T. would like to thank Gaussian, Inc. for financial support.

References and Notes

(1) Glasel, J. A. Nuclear Magnetic Resonance Studies on Water and Ice. In *Water: A Comprehensive Treatise*; Franks, F., Ed.; Plenum Press: New York & London, 1982; Vol. 1, Chapter 6, p 223. Fister, F.; Hertz, H. G. *Ber. Bunsen-Ges. Phys. Chem.* **1987**, *71*, 1032. Hertz, H. G.; Maurer, R.; Killie, S. Z. *Z. Phys. Chem.* **1991**, *172*, 157. Luz, Z.; Yagil, G. *J. Phys. Chem.* **1966**, *70*, 554. Wasylishen, R. E.; Mooibroek, S.; Macdonald, J. B. *J. Chem. Phys.* **1984**, *81*, 1057. Wu, G.; Hook, A.; Dong, S.; Yamada, K. *J. Phys. Chem. A* **2000**, *104*, 4102. Pfrommer, B. G.; Mauri, F.; Louie, S. G. *J. Am. Chem. Soc.* **2000**, *122*, 123.

(2) Bernal, J. D.; Fowler, R. H. *J. Chem. Phys.* **1933**, *1*, 515.

(3) Helgaker, T.; Jaszunski, M.; Ruud, K. *Chem. Rev.* **1999**, *99*, 293.

(4) Mikkelsen, K. V.; Ruud, K.; Helgaker, T. *Chem. Phys. Lett.* **1996**, *253*, 443. Mikkelsen, K. V.; Jørgensen, P.; Ruud, K.; Helgaker, T. *J. Chem. Phys.* **1997**, *106*, 1170. Cammi, R. *J. Chem. Phys.* **1998**, *109*, 3185. Cammi, R.; Mennucci, B.; Tomasi, J. *J. Chem. Phys.* **1999**, *110*, 7627.

(5) Svishchev, I. M.; Kusalik, P. G. *J. Am. Chem. Soc.* **1993**, *115*, 8270. Nymand, T. M.; Åstrand, P.-O.; Mikkelsen, K. V. *J. Phys. Chem. B* **1997**, *101*, 4105. Pfrommer, B. G.; Mauri, F.; Louie, S. G. *J. Am. Chem. Soc.* **2000**, *122*, 123. Cui, Q.; Karplus, M. *J. Phys. Chem. B* **2000**, *104*, 3721.

(6) Tomasi, J.; Cammi, R.; Mennucci, B.; Cappelli, C.; Corni, S. *Phys. Chem. Chem. Phys.* **2002**, *4*, 5697.

(7) Mennucci, B. *J. Am. Chem. Soc.* **2002**, *124*, 1506.

(8) Mennucci, B.; Martínez, J. M.; Tomasi, J. *J. Phys. Chem. A* **2001**, *105*, 7287.

(9) Chesnut, D. B.; Rusiloski, B. E. *J. Mol. Struct. (THEOCHEM)* **1994**, *314*, 19. Malkin, V. G.; Malkina, O. L.; Steinebrunner, G.; Huber, H. *Chem.-Eur. J.* **1996**, *2*, 452. Cui, Q.; Karplus, M. *J. Phys. Chem. B* **2000**, *104*, 3721.

(10) Cossi, M.; Crescenzi, O. *J. Chem. Phys.* **2003**, *118*, 8863.

(11) Chesnut, D. B. *J. Phys. Chem. A* **2002**, *106*, 6876. Yamazaki, T.; Sato, H.; Hirata, F. *Chem. Phys. Lett.* **2000**, *325*, 668.

(12) Cramer, C. J. *Essentials of Computational Chemistry*; John Wiley & Sons: Chichester, UK, 2002; Vol. 11, p 373.

(13) Pfrommer, B. G.; Mauri, F.; Louie, S. G. *J. Am. Chem. Soc.* **2000**, *122*, 123.

(14) Car, R.; Parrinello, M. *Phys. Rev. Lett.* **1985**, *55*, 2471.

(15) Frank, H. S. *Science* **1970**, *169*, 635. Frank, H. S. *Water*; Plenum Press: New York, 1975; Vols. 1−5. Stillinger, F. H. *Science* **1980**, *207*, 451. Rahman, A.; Stillinger, F. H. *J. Am. Chem. Soc.* **1973**, *95*, 7943. Stillinger, F. H.; Rahman, A. *J. Chem. Phys.* **1974**, *60*, 1545.

(16) Soper, A. K.; Phillips, M. G. *Chem. Phys.* **1986**, *107*, 47. Soper, A. K.; Bruni, F.; Ricci, M. A. *J. Chem. Phys.* **1997**, *106*, 247.

(17) Finney, J. L.; Hallbrucker, A.; Kohl, I.; Soper, A. K.; Bowron, D. T. *Phys. Rev. Lett.* **2002**, *88*, 225503. Koh, C. A.; Wisbey, R. P.; Wu, X.; Westacott, R. E.; Soper, A. K. *J. Chem. Phys.* **2000**, *113*, 6390. English, N. J.; Macelroy, J. M. D. *J. Comput. Chem.* **2003**, *24*, 1569.

(18) Frisch, M. J.; Trucks, G. W.; Schlegel, H. B.; Scuseria, G. E.; Robb, M. A.; Cheeseman, J. R.; Zakrzewski, V. G.; Montgomery, J. A., Jr.; Stratmann, R. E.; Burant, J. C.; Dapprich, S.; Millam, J. M.; Daniels, A. D.; Kudin, K. N.; Strain, M. C.; Farkas, O.; Tomasi, J.; Barone, V.; Cossi, M.; Cammi, R.; Mennucci, B.; Pomelli, C.; Adamo, C.; Clifford, S.; Ochterski, J.; Petersson, G. A.; Ayala, P. Y.; Cui, Q.; Morokuma, K.; Salvador, P.; Dannenberg, J. J.; Malick, D. K.; Rabuck, A. D.; Raghavachari, K.; Foresman, J. B.; Cioslowski, J.; Ortiz, J. V.; Baboul, A. G.; Stefanov, B. B.; Liu, G.; Liashenko, A.; Piskorz, P.; Komaromi, I.; Gomperts, R.; Martin, R. L.; Fox, D. J.; Keith, T.; Al-Laham, M. A.; Peng, C. Y.; Nanayakkara, A.; Challacombe, M.; Gill, P. M. W.; Johnson, B.; Chen, W.; Wong, M. W.; Andres, J. L.; Gonzalez, C.; Head-Gordon, M.; Replogle, E. S.; Pople, J. A. *Gaussian 98*, revision A.11; Gaussian, Inc.: Pittsburgh, PA, 2001.

(19) Frisch, M. J.; Trucks, G. W.; Schlegel, H. B.; Scuseria, G. E.; Robb, M. A.; Cheeseman, J. R.; Montgomery, J. A., Jr.; Vreven, T.; Kudin, K. N.; Burant, J. C.; Millam, J. M.; Iyengar, S. S.; Tomasi, J.; Barone, V.; Mennucci, B.; Cossi, M.; Scalmani, G.; Rega, N.; Petersson, G. A.; Nakatsuji, H.; Hada, M.; Ehara, M.; Toyota, K.; Fukuda, R.; Hasegawa, J.; Ishida, M.; Nakajima, T.; Honda, Y.; Kitao, O.; Nakai, H.; Klene, M.; Li, X.; Knox, J. E.; Hratchian, H. P.; Cross, J. B.; Adamo, C.; Jaramillo, J.; Gomperts, R.; Stratmann, R. E.; Yazyev, O.; Austin, A. J.; Cammi, R.; Pomelli, C.; Ochterski, J. W.; Ayala, P. Y.; Morokuma, K.; Voth, G. A.; Salvador, P.; Dannenberg, J. J.; Zakrzewski, V. G.; Dapprich, S.; Daniels, A. D.; Strain, M. C.; Farkas, O.; Malick, D. K.; Rabuck, A. D.; Raghavachari, K.; Foresman, J. B.; Ortiz, J. V.; Cui, Q.; Baboul, A. G.; Clifford, S.; Cioslowski, J.; Stefanov, B. B.; Liu, G.; Liashenko, A.; Piskorz, P.; Komaromi, I.; Martin, R. L.; Fox, D. J.; Keith, T.; Al-Laham, M. A.; Peng, C. Y.; Nanayakkara, A.; Challacombe, M.; Gill, P. M. W.; Johnson, B.; Chen, W.; Wong, M. W.; Gonzalez, C.; Pople, J. A. *Gaussian 03*, revision A.1; Gaussian, Inc.: Pittsburgh, PA, 2003.

(20) *NBO 5.0*; Glendening, E. D.; Badenhoop, J. K.; Reed, A. E.; Carpenter, J. E.; Bohmann, J. A.; Morales, C. M.; Weinhold, F. Theoretical Chemistry Institute, University of Wisconsin, Madison, WI, 2001.

(21) Klein, R. A. *J. Comput. Chem.* **2002**, *23*, 585.

(22) Klein, R. A. *J. Am. Chem. Soc.* **2002**, *124*, 13931.

(23) Klein, R. A. *J. Comput. Chem.* **2003**, *24*, 1120.

(24) Biegler-König, F. H. *J. Comput. Chem.* **2000**, *21*, 1040. Biegler-König, F. H.; Schönbohm, J.; Bayles, D. *J. Comput. Chem.* **2001**, *22*, 545. Biegler-König, F. W.; Bader, R. W. F.; Tang, T. H. *J. Comput. Chem.* **1982**, *3*, 317.

(25) MORPHY98, a topological analysis program written by P. L. A. Popelier with a contribution from R. G. A. Bone (UMIST, Manchester, England). Popelier, P. L. A. *Comput. Phys. Commun.* **1996**, *93*, 212. Popelier, P. L. A. *Theor. Chim. Acta* **1994**, *87*, 465. Popelier, P. L. A. *Mol. Phys.* **1996**, *87*, 1169. Popelier, P. L. A. *Comput. Phys. Commun.* **1998**, *108*, 180. Popelier, P. L. A. *Can. J. Chem.* **1996**, *74*, 829.

(26) Ditchfield, R. *Mol. Phys.* **1974**, *27*, 789.

(27) Sum, A. K.; Burruss, R. C.; Sloan, E. D. *J. Phys. Chem. B* **1997**, *101*, 7371. Sparks, K. A.; Tester, J. W.; Cao, Z.; Trout, B. L. *J. Phys. Chem. B* **1999**, *103*, 6300. Gutt, C.; Asmussen, B.; Press, W.; Johnson, M. R.; Handa, Y. P.; Tse, J. S. *J. Chem. Phys.* **2000**, *113*, 4713.

(28) Vaara, J.; Lounila, J.; Ruud, K.; Helgaker, T. *J. Chem. Phys.* **1998**, *109*, 8388.

(29) Bohmann, J. A.; Weinhold, F.; Farrar, T. C. *J. Chem. Phys.* **1997**, *107*, 1173.

(30) Haeberlen, U. In *Advances in Magnetic Resonance*; Waugh, J. S., Ed.; Academic Press: New York, 1976; Suppl. 1. Mehring, M. *Principles of High-Resolution NMR in Solids*, 2nd ed.; Springer-Verlag: Berlin, 1983. Spiess, H. W. In *NMR Basic Principles and Progress*; Diehl, P., Fluck, E., Kosfeld, R., Eds.; Springer-Verlag: Berlin, 1978; Vol. 15.

(31) Buckingham, A. D. *Q. Rev. Chem. Soc.* **1959**, *13*, 183.

(32) Wiberg, K. B.; Rablen, P. R. *J. Comput. Chem.* **1993**, *14*, 1504.

(33) Bader, R. F. W. In *Atoms in Molecules. A Quantum Theory*; International Series of Monographs on Chemistry No. 22; Rowlinson, J. S., Green, M. L. H., Halpern, J., Ley, S. V., Mukaiyama, T., Schowen, R. L., Thomas, J. M., Zewail, A. H., Eds.; Oxford University Press: Oxford, UK, 1990.

(34) Stone, A. J. *Chem. Phys. Lett.* **1981**, *83*, 233. Stone, A. J.; Alderton, M. *Mol. Phys.* **1985**, *56*, 1047.

(35) Guerra, C. F.; Handgraaf, J.-W.; Baerends, E. J.; Bickelhaupt, F. M. *J. Comput. Chem.* **2003**, *25*, 189.

(36) Halle, B.; Wennerstrom, H. *J. Phys. Chem.* **1981**, *75*, 1928. Halle, B.; Piculell, L. *J. Chem. Soc., Faraday Trans. 1* **1982**, *78*, 255. Ludwig, R. *Chem. Phys.* **1995**, *195*, 329.

(37) Cancès, E.; Mennucci, B.; Tomasi, J. *J. Chem. Phys.* **1997**, *107*, 3032. Miertus, S.; Scrocco, E.; Tomasi, J. *Chem. Phys.* **1981**, *55*, 117. Cammi, R.; Tomasi, J. *J. Comput. Chem.* **1995**, *16*, 1449.

(38) Cammi, R. *J. Chem. Phys.* **1998**, *109*, 3185. Cammi, R.; Mennucci, B.; Tomasi, J. *J. Chem. Phys.* **1999**, *110*, 7627.

(39) Yamazaki, T.; Sato, H.; Hirata, F. *Chem. Phys. Lett.* **2000**, *325*, 668.

(40) Hoffmann, M. M.; Conradi, M. S. *J. Am. Chem. Soc.* **1997**, *119*, 3811. Bellissent-Funel, M.-C. *J. Mol. Liq.* **2001**, *90*, 313.

(41) Feyereisen, M. W.; Feller, D.; Dixon, D. A. *J. Phys. Chem.* **1996**, *100*, 2993.

(42) Stillinger, F. H. *Science* **1980**, *207*, 451. Kalinichev, A. G.; Bass, J. D. *J. Phys. Chem. A* **1997**, *101*, 9720. Soper, A. K.; Bruni, F.; Ricci, M. A. *J. Chem. Phys.* **1997**, *106*, 247.

(43) Klein, R. A.; Pacheco, V. *J. Phys. Chem. A* **2001**, *105*, 9298.

(44) Jorgensen, W. L.; Chandrasekhar, J.; Madura, J. D.; Impey, R. W.; Klein, M. L. *J. Chem. Phys.* **1983**, *79*, 926. Berendsen, H. J. C.; Grigera, J. R.; Straatsma, T. P. *J. Phys. Chem.* **1987**, *91*, 6269. Stillinger, F. H.; Rahman, A. *J. Chem. Phys.* **1974**, *60*, 1545. Mahoney, M. W.; Jorgensen, W. L. *J. Chem. Phys.* **2000**, *112*, 8910. Mahoney, M. W.; Jorgensen, W. L. *J. Chem. Phys.* **2001**, *114*, 363. Mahoney, M. W.; Jorgensen, W. L. *J. Chem. Phys.* **2001**, *115*, 10758. Lisal, M.; Kolafa, J.; Nezbeda, I. *J. Chem. Phys.* **2002**, *117*, 8892. Rick, S. W.; Stuart, S. J.; Berne, B. J. *J. Chem. Phys.* **1994**, *101*, 6141. Niesar, U.; Corongiu, G.; Clementi, E.; Keller, G. R.; Bhattacharya, D. K. *J. Phys. Chem.* **1990**, *94*, 7949. Corongiu, G. *Int. J. Quantum Chem.* **1992**, *42*, 1209.

(45) Tomasi, J.; Cammi, R.; Mennucci, B.; Cappelli, C.; Corni, S. *Phys. Chem. Chem. Phys.* **2002**, *4*, 5697.